Estimation of Interior Temperature Distribution of Work in Laser Materials Processing Using IR Camera (Report 1)†

Katsunori INOUE*, Etsuji OHMURA**, Ling-Jun GAO*** and Na YI****

Abstract

In this paper, a simple measuring system is constructed to estimate the quasi-steady state temperature distribution in the work under CW CO_2 laser irradiation. This system is composed of an infrared camera, a video recorder, an image processor and a personal computer. The surface temperature of the work is measured by an IR camera, and computation based on a semi-analytical solution derived using Green's function is carried out by a personal computer. This system is applied to an actual laser materials processing experimentally to confirm efficiency of this system.

KEY WORDS: (Laser Materials Processing) (Temperature Measuring System) (IR Camera) (Heat Conduction)

1. Introduction

In recent years, CW CO_2 lasers are being introduced in manufacturing process in many factories[1]. Controlling the laser irradiating conditions[2] and quality control of the products present important subjects for laser materials processing. Interior temperature of the work under laser irradiation gives a beneficial information for these control[3),4]. It is very difficult to measure the temperature distribution in the work directly by thermocouple, resistance thermometer or radiation pyrometer during laser irradiation process. On the other hand, it is relatively easy to measure the surface temperature distribution on the work using an infrared camera[5] even under laser irradiation.

If the surface temperature is given in the form of a function, the interior temperature of a solid can be estimated theoretically. The solution can be derived using Green's function. The information obtained by an IR camera is usually processed using an image processor, and the data are given discretely. In this paper, an analytical equation of the interior temperature is expressed in discretized form, and computation based on this semi-analytical solution is carried out by a personal computer using the surface temperature distribution obtained by an IR camera. This measuring system is applied to a laser materials processing experimentally, and the interior temperature distribution is estimated actually to confirm efficiency of this system.

2. Analysis

Figure 1 shows the semi-infinite solid which is traveling toward the direction of x positive at a constant speed v. Let T be the temperature at the time t in the solid due to the surface temperature $\Psi(x, y, t)$ and zero initial temperature. Then T satisfies the equations

$$\frac{\partial T}{\partial t} = a\nabla^2 T - v\frac{\partial T}{\partial x}, \tag{1}$$

$$T = 0 \text{ initially, in } z > 0, \tag{2}$$

and

$$T = \Psi(x, y, t), \text{ at } z = 0, \text{ when } t > 0. \tag{3}$$

In this case, the Green's function is

$$G(x, y, z, t; \xi, \eta, \zeta, \tau) = \frac{1}{\{4\pi a(t-\tau)\}^{3/2}} \exp\left[-\frac{\{x-\xi-v(t-\tau)\}^2+(y-\eta)^2}{4a(t-\tau)}\right] \times\left[\exp\left\{-\frac{(z-\zeta)^2}{4a(t-\tau)}\right\}-\exp\left\{-\frac{(z+\zeta)^2}{4a(t-\tau)}\right\}\right], \tag{4}$$

where a is the thermal diffusivity of the solid, and T is given by[6]

† Received on Apr. 28, 1986.

* Professor
** Research Instructor
*** Co-operative Researcher (Senior Engineer, Beijing Research Institute of Material and Technology)
**** Co-operative Researcher (Engineer, Beijing Research Institute of Material and Technology)

Transactions of JWRI is published by Welding Research Institute of Osaka University, Ibaraki, Osaka 567, Japan

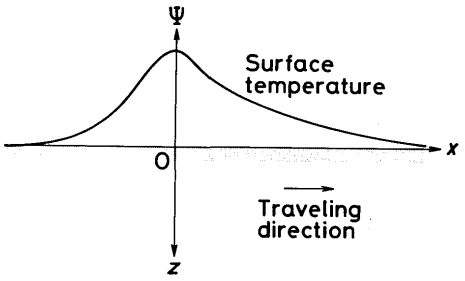

Fig. 1 Coordinate system.

$$T(x,y,z,t) = a\int_0^t\int_{-\infty}^{\infty}\int_{-\infty}^{\infty}\Psi(\xi,\eta,\tau)\frac{\partial G}{\partial\zeta}(x,y,z,t;\xi,\eta,0,\tau)d\xi d\eta d\tau. \tag{5}$$

Substituting Eq. (4) into Eq. (5), we obtain

$$T(x,y,z,t) = \frac{z}{(4\pi a)^{3/2}}\int_0^t\int_{-\infty}^{\infty}\int_{-\infty}^{\infty}\frac{\Psi(\xi,\eta,\tau)}{(t-\tau)^{5/2}} \times \exp\left[-\frac{\{x-\xi-v(t-\tau)\}^2+(y-\eta)^2+z^2}{4a(t-\tau)}\right]d\xi d\eta d\tau. \tag{6}$$

When the surface temperature is kept constant all the time and symmetric with respect to the x axis, the quasi-steady state temperature is obtained as follows:

$$T(x,y,z) = \frac{z}{(4\pi a)^{3/2}}\int_0^{\infty}\int_{-\infty}^{\infty}\int_{-\infty}^{\infty}\frac{\Psi(\xi,\eta)}{\tau^{5/2}} \times \exp\left\{-\frac{(x-\xi-v\tau)^2+(y-\eta)^2+z^2}{4a\tau}\right\}d\xi d\eta d\tau. \tag{7}$$

The plane $z = 0$ will be divided into fine segments whose size is $\Delta x \times \Delta y$. The surface temperature is assumed to be constant on each segment and equal to the value at the center of the segment. Eq. (4) can be expressed in discretized form

$$T(x,y,z) = \frac{z\Delta x\Delta y}{(4\pi a)^{3/2}}\sum_{i=-\infty}^{\infty}\sum_{j=0}^{\infty}\Psi(x_i,y_j)\int_0^{\infty}\frac{1}{\tau^{5/2}} \times \exp\left\{-\frac{(x-x_i-v\tau)^2+z^2}{4a\tau}\right\} \times\left[\exp\left\{-\frac{(y-y_j)^2}{4a\tau}\right\}+\exp\left\{-\frac{(y+y_j)^2}{4a\tau}\right\}\right]d\tau, \tag{8}$$

where (x_i, y_j) is the coordinates of the center of the (i, j) segment.

3. Numerical Computations

In order to examine the discretized equation (8) for validity, the results obtained by Eq. (8) are compared with analytical solution for the case in which the surface temperature is Gaussian distribution given by

$$\Psi(x,y) = \Psi_0\exp\left\{-\frac{1}{r_0^2}(x^2+y^2)\right\}, \tag{9}$$

where r_0 is the radius at which the temperature is reduced from the center value Ψ_0 by a factor of e^2. Substituting Eq. (9) into Eq. (6), the analytical solution is obtained as follows:

$$T(x,y,z) = \frac{r_0^2 z\Psi_0}{2\sqrt{\pi a}}\int_0^{\infty}\frac{1}{\tau^{3/2}(8a\tau+r_0^2)} \times\exp\left\{-\frac{2(x-v\tau)^2+2y^2}{8a\tau+r_0^2}-\frac{z^2}{4a\tau}\right\}d\tau. \tag{10}$$

Figure 2 shows the results of numerical computations

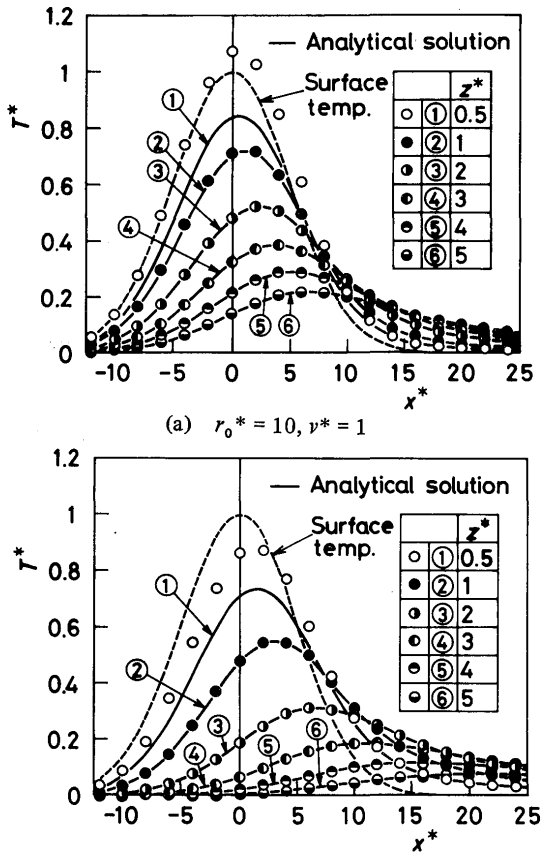

Fig. 2 Comparison between semi-analytical and analytical solutions for the case in which the surface temperature is Gaussian distribution.

on the plane $y = 0$ obtained by Eqs. (8) and (10), where

$$T^* = \frac{T}{\Psi_0}, x^* = \frac{x}{\Delta x}, z^* = \frac{z}{\Delta x}, r_0{}^* = \frac{r_0}{\Delta x},$$

$$v^* = \frac{v\Delta x}{a}. \quad (11)$$

The combination of $i = 0, \pm1, \pm2, \cdots, \pm23$ and $j = 0, 1, 2, \cdots, 23$ is used for the double series in Eq. (8), and Δy is taken to be equal to the value Δx. The discretized solution, which is shown by circles, agrees well with analitical solution below $z^* = 1$, and it is concluded that Eq. (8) is effective in the area below the depth which is equal to the larger value of Δx and Δy. It is the reason why the difference between these two solutions increases near the surface that contribution of only the center point (x_i, y_j) of each segment on the surface to an interior point (x, y, z) is considered in Eq. (8). If contributions of all points on each segment to an interior point are considered, the semi-analytical solution will agree better with analytical solution.

4. Measuring System

The system is composed mainly of an infrared camera, a video recorder, an image processor and a personal computer as shown in **Fig. 3**. The radiation intensity distribution on the surface of the work is measured by an IR camera and the output signal is recorded by a video recorder. The IR camera used is the Model 525 Infrared Scanner made by Inframetrics, Inc., whose frame rate is 30 Hz with 2 : 1 interlace. This infrared detector is a liquid-nitrogen-cooled HgCdTe quantum detector. The brightness of pictures obtained, which corresponds to the radiation intensity, is analyzed by an image processor, TVIP2000 made by Nippon Avionics Co., Ltd., and transformed into temperature by a personal computer using the isotherm calibration curves. The emmisivity is also considered in this transformation. The surface temperature is stored in a floppy disk for the time being, and computation based on the semi-analytical solution, that is, Eq. (8) in Ch. 1 is carried out by the personal computer using the surface temperature distribution obtained.

5. Experiments and Results

Figure 4 shows the optical system for CO_2 laser to obtain a rectangular intensity distribution of heat source and the IR camera position. The laser irradiating condition is shown in **Table 1**. The workpiece is a plate of width 50 mm, length 150 mm and thickness 15 mm, and

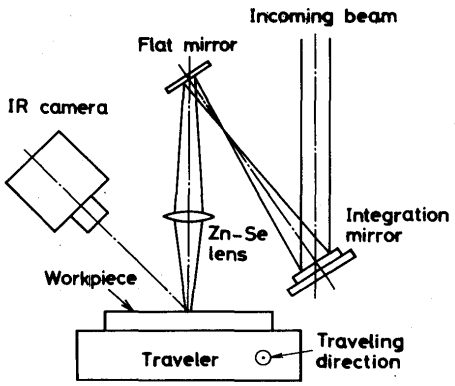

Fig. 4 Schematic illustration of the optical system for CO_2 laser to obtain a rectangular intensity distribution of heat source and the IR camera position.

Table 1 Laser irradiating conditions.

Laser power	Beam size	Traveling velocity
1.2 kW	3.9 mm×3.9 mm	20 mm/s

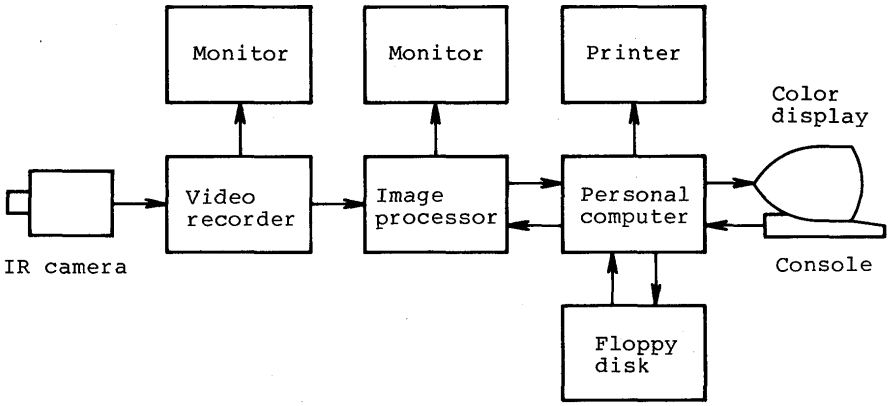

Fig. 3 Block diagram of the measuring system to estimate the quasi-steady state temperature distribution in the work under CW CO_2 laser irradiation.

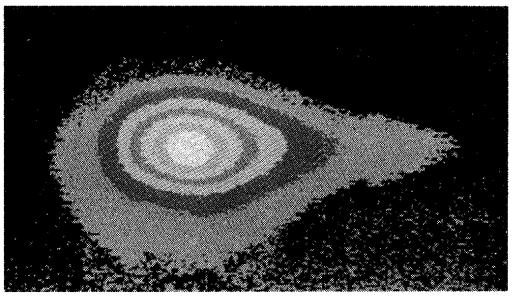

Fig. 5 Original image of surface temperature distribution in a quasi-steady state displayed on the color display after the radiation intensity is transfered into temperature by the personal computer.

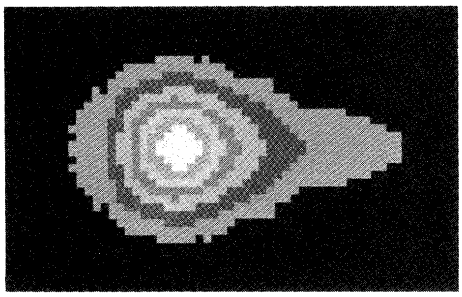

Fig. 6 Surface temperature distribution after noise reduction and correction of the camera angle. The surface temperature on both areas $y > 0$ and $y < 0$ is averaged.

the work material is carbon steel S45C which is equivalent to AISI 1045. The phosphate treatment is performed on the surface to improve the absorptance for the laser beam.

Figure 5 shows the surface temperature distribution in a quasi-steady state displayed on the color display after the radiation intensity is transformed into temperature by the personal computer. This image is expressed by 8 color codes between the maximum temperature and the room temperature. The angle between the optical axis of the IR camera and the workpiece surface to be measured is not corrected yet, and a little noise is noticed in this figure.

Figure 6 shows the same surface temperature distribution after the continuous 4 frames obtained by the IR camera are averaged on the image processor to reduce the noise and the camera angle is also corrected. The size of one segment is 0.5 mm × 0.5 mm. The temperature distribution is nearly symmetric with respect to the plane $y = 0$, that is, the plane which contains the center of the heat source as shown in Fig. 5. Therefore, the surface temperature on both areas $y > 0$ and $y < 0$ is averaged on the personal computer. This temperature distribution is illustrated by isothermal lines in **Fig. 7**, where the origin is taken at the maximum temperature on the surface. The surface temperature is higher than the room temperature

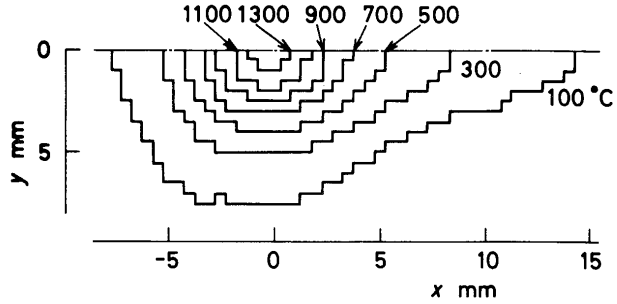

Fig. 7 The same temperature distribution as Fig. 6 illustrated by isothermal lines.

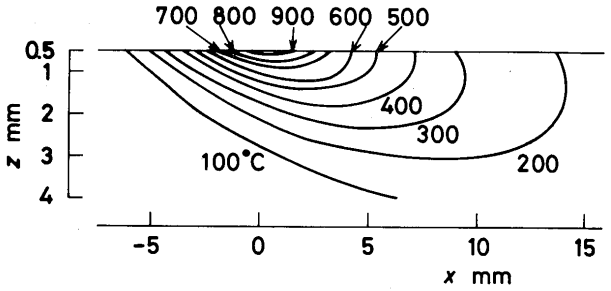

Fig. 8 Temperature distribution on the plane $y = 0$ under the laser irradiating conditions in Table 1.

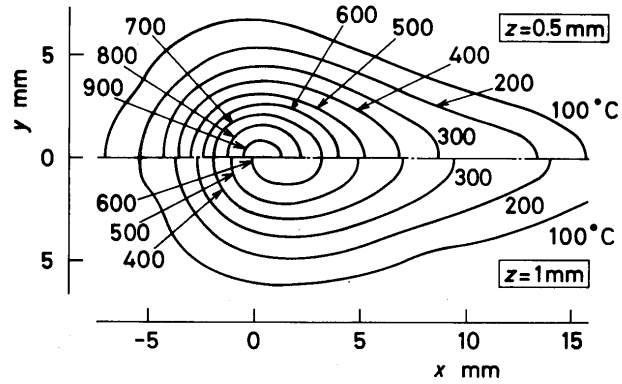

Fig. 9 Temperature distribution on both planes z = 0.5 mm and z = 1 mm under the laser irradiating conditions in Table 1.

at $-9.5 \text{ mm} \leqslant x \leqslant 16 \text{ mm}$ and $0 \leqslant y \leqslant 8.5$ mm in Fig. 7.

The estimated results on the interior temperature distribution are shown in **Figs. 8** and **9**. Figure 8 shows the temperature distribution on the plane $y = 0$. The temperature distribution on both planes $z = 0.5$ mm and 1 mm is shown in Fig. 9. These results can be used to get the information of heating or cooling rate, phase transformation, molten zone, etc. The surface temperature obtained at the rear of the heat source, that is, in $x > 0$ area decreases more rapidly than the analytical solution in heat source problem[4] and there is a little difference in the form of the isothermal lines in $x > 0$ area between the estimated results in Fig. 8 and the results obtained by analysis for heat source problem.

6. Conclusion

An analytical solution to estimate the interior temperature distribution of a semi-infinite solid which is traveling at a constant speed under laser irradiation was derived using Green's function. This solution was expressed in discretized form. A simple measuring system was constructed, which was composed of an infrared camera, a video recorder, an image processor and a personal computer. This system was applied to an actual laser materials processing experimentally, and the interior temperature distribution was expressed by isothermal lines on some planes. It will be also able to estimate the heating or cooling rate of the work in laser materials processing using these results.

If this measuring system is applied to the manufacturing process in which CO_2 lasers are introduced, it will be very useful in controlling the laser irradiating conditions or for quality control of the products.

References

1) Luxon, J.T. and Parker, D.E., *Industrial Lasers and Their Applications*, Prentice-Hall, (1985).

2) Ohmura, E., Namba, Y. and Makinouchi, S., *Trans. Japan Soc. Mech. Engrs.* (Ser. C), Vol. 51, No. 469, p. 2373 (1985) (in Japanese).

3) Ohmura, E., Namba, Y. and Makinouchi, S., *Bull. JSME*, vol. 26, No. 219, p. 1670 (1983).

4) Kou, S., Sun, D.K. and Le, Y.P., *Metallug. Trans.* A, Vol. 14A, No. 4, p. 643 (1983).

5) Kaplan, H., *Laser Focus*, Vol. 20, No. 3, p. 57 (1984).

6) Snnedon, I.N., *Elements of Partial Differential Equations*, McGrall-Hill, p. 294 (1957).